Mon. Not. R. astr. Soc. (1972) **156,** 437–458.

THE COLLAPSE OF A ROTATING CLOUD

Richard B. Larson

(Received 1971 October 13)

SUMMARY

Numerical calculations have been made for the early stages of collapse of an axisymmetric cloud, both with and without rotation. The results show that, in the absence of rotation, deviations from spherical symmetry do not usually grow as the cloud collapses; instead, pressure forces remain sufficient to maintain rough spherical symmetry and prevent the cloud from fragmenting during its collapse. Fragmentation can occur, but usually only if the initial configuration is already unstable to fragmentation. In the presence of rapid rotation, however, the central part of the cloud always appears to condense into a rotating ' doughnut ' or ring with a density minimum at the centre. Such a rotating ring is almost certainly unstable and will presumably fragment into two or more condensations orbiting around each other. The formation in this way of a binary or multiple system of stars would largely resolve the classical ' angular momentum problem ' and might account for the fact that most stars are in fact found in binary or multiple systems; even the single stars might be accounted for as escapers from unstable multiple systems.

1. INTRODUCTION

In recent years a number of authors have calculated the early stages of the collapse of a spherically symmetric, non-rotating gas cloud (Bodenheimer & Sweigart 1968; Hunter 1969; Larson 1969; Penston 1969; Disney, McNally & Wright 1969; for a brief review see Penston 1971). Despite considerable differences in the assumptions adopted by the various authors, there is substantial agreement concerning the major features of the collapse. At the high densities ($\gtrsim 10^{-21}$ g cm^{-3}) required for the collapse of a protostellar cloud with mass in the normal stellar mass range, cooling mechanisms are very efficient and maintain the temperature almost constant at a value of the order of 10 to 20°K; the cloud therefore collapses essentially isothermally until the central part of the cloud becomes opaque to infra-red radiation, which occurs at a density of the order of 10^{-13} g cm^{-3}. The collapse is always found to be extremely non-homologous and the density distribution rapidly becomes very sharply peaked at the centre, the density law being approximately of the form $\rho \propto r^{-2}$. This non-homologous character of the collapse is of great importance for the later development of the protostar (Larson 1969; Larson & Starrfield 1971).

It is evident, however, that the assumption of spherical symmetry which has characterized all calculations up to the present is a rather strong idealization, since there is no *a priori* reason to expect a collapsing cloud to maintain spherical symmetry; in fact, there are arguments which suggest that the assumption of spherical symmetry may be a poor one. It is known, for example, that if a uniform, pressure-free spheroid collapses gravitationally, its eccentricity increases steadily during the collapse (Lynden-Bell 1964; Mestel 1965a); the calculations of Lin, Mestel & Shu

(1965) show that an oblate spheroid rapidly flattens to a disc, and a prolate spheroid collapses to a line. The flattening of an oblate spheroid will be inhibited if finite pressure gradients are included, but Mestel (1965a) has argued that the eccentricity will still continue to increase indefinitely as the collapse proceeds. For a prolate or cylindrical mass distribution, even the inclusion of finite pressure gradients cannot prevent collapse to an infinitely thin cylinder if the mass per unit length exceeds a certain critical value. These results suggest that a spherically symmetric collapsing cloud will be unstable to the growth of both oblate and prolate deformations from spherical symmetry. In order to investigate this question by numerical calculations, it is clearly necessary to relax the assumption of spherical symmetry and compute the collapse of an axially symmetric cloud.

A related question which cannot be answered by spherical collapse calculations is whether an isothermally collapsing cloud will tend to fragment into smaller condensations during its collapse. While it is generally believed that fragmentation does frequently occur, the process of fragmentation remains poorly understood, despite much discussion (Mestel 1965a, b; Hunter 1967; Arny 1967). Since fragmentation constitutes a deviation from spherical symmetry, any tendency toward fragmentation will be suppressed in calculations which assume spherical symmetry throughout the collapse. To study the fragmentation problem numerically, it would be desirable to undertake a full three-dimensional calculation, and it is not clear *a priori* that much can be learned from an axisymmetric (two-dimensional) calculation; nevertheless, this at least represents a first step in relaxing the assumption of spherical symmetry.

Our primary reason for studying the collapse of an axially symmetric cloud has been to investigate the effect of rotation on the collapse. The effect of rotation has been a long-standing bugaboo in the theory of star formation. It has frequently been pointed out, for example, that if a protostellar cloud begins its collapse with an angular velocity comparable with that of galactic rotation, its angular momentum is far too large to allow it to collapse into a star. Because of this, it has usually been thought that angular momentum must somehow be removed from the cloud during its collapse, and magnetic fields have often been invoked for this purpose (see, for example, Mestel 1965b). The assumption that the initial rotation of the cloud is related to galactic rotation may be questioned, since neither stellar rotation axes nor the axes of binary systems show any preferential orientation perpendicular to the galactic plane (cf. also Disney *et al.* 1969). The observed random orientation of rotation axes suggests that the rotational motions may have originated in random turbulent motions in the interstellar medium; in this case, the rotational velocities of protostellar clouds would be expected to be comparable with their translational velocities, which would lead to angular velocities even *higher* than that of galactic rotation. The effect of rotation would then be even more important than previously believed. In any case, it seems difficult to escape the conclusion that for most protostellar clouds the effects of rotation must become important at an early stage in the collapse, long before stellar conditions are reached.

In this paper we report the results of a first crude attempt to compute numerically the collapse of an axisymmetric gas cloud, assuming a variety of initial conditions, both with and without rotation. Because the possible role of magnetic fields in the collapse of a protostar is still quite uncertain, and since the inclusion of their effects would greatly complicate the calculations, we have neglected magnetic fields, as well as other possible sources of viscosity. The following section

outlines the equations and assumptions which have been employed in these calculations, and Sections 3 and 4 give the results for non-rotating and rotating clouds respectively. The implications of these results for our understanding of star formation and fragmentation are discussed in Section 5.

2. EQUATIONS AND ASSUMPTIONS

The present calculations have been intended to represent, as nearly as possible, a generalization to two dimensions of the calculations already made for the collapse of a spherical protostar (Larson 1969). Consequently, we have adopted the same assumptions as before concerning the composition and opacity of the protostellar material. During the initial optically thin stages of the collapse, the collapsing cloud remains very nearly isothermal, and a temperature of 10°K has usually been assumed, as in the spherical calculations. Also, we have adopted the same boundary conditions as before, i.e. a spherical boundary fixed in space. In the spherical case, it is well documented from the results of several investigations that the exact choice of boundary condition makes little difference to the gross features of the collapse. In the present case, it may seem restrictive to impose a spherical boundary on a cloud whose internal density distribution is not spherical; however, we find in these calculations that the most significant developments, including the largest deviations from spherical symmetry, always tend to occur near the centre of the cloud, i.e. well away from the boundary, so that the influence of the boundary condition should not be very important.

The present calculations have all been made for a cloud with a mass of one solar mass, and the radius has in most cases been set equal to 10^{17} cm. This radius is somewhat smaller than the value of $1{\cdot}63 \times 10^{17}$ cm used in the spherical calculations (Larson 1969); the reason for this, as will be explained more fully in Section 4, is that when the cloud is rotating, it must be compressed somewhat more than a non-rotating cloud in order for gravity to overcome the combined effects of pressure and centrifugal forces and cause the cloud to collapse. Since the cloud remains isothermal during the early stages of the collapse, with which this paper is primarily concerned, the results can be scaled to other values of the mass, radius, and temperature as long as the ratio M/RT is kept constant.

The numerical calculations have been made using an Eulerian grid with spherical polar coordinates r, θ, ϕ, where the azimuthal coordinate ϕ does not appear explicitly in the calculations because of the assumption of axial symmetry. Accordingly, we give below the Eulerian equations of inviscid gas dynamics expressed in spherical polar coordinates. Denoting by u, v and w the velocity components in the r, θ and ϕ directions respectively, and denoting by Φ the gravitational potential, we have

$$\frac{\partial \rho}{\partial t}+\frac{1}{r^2}\frac{\partial}{\partial r}(r^2\rho u)+\frac{1}{r\sin\theta}\frac{\partial}{\partial \theta}(\sin\theta\,\rho v)=0 \tag{1}$$

$$\frac{\partial u}{\partial t}+u\frac{\partial u}{\partial r}+\frac{v}{r}\frac{\partial u}{\partial \theta}+\frac{1}{\rho}\frac{\partial P}{\partial r}+\frac{\partial \Phi}{\partial r}-\frac{v^2+w^2}{r}=0 \tag{2}$$

$$\frac{\partial v}{\partial t}+\frac{u}{r}\frac{\partial}{\partial r}(rv)+\frac{v}{r}\frac{\partial v}{\partial \theta}+\frac{1}{\rho r}\frac{\partial P}{\partial \theta}+\frac{1}{r}\frac{\partial \Phi}{\partial \theta}-\frac{w^2}{r\tan\theta}=0 \tag{3}$$

$$\frac{\partial w}{\partial t}+\frac{u}{r}\frac{\partial}{\partial r}(rw)+\frac{v}{r\sin\theta}\frac{\partial}{\partial \theta}(\sin\theta\,w)=0 \tag{4}$$

$$\frac{\partial E}{\partial t}+u\frac{\partial E}{\partial r}+\frac{v}{r}\frac{\partial E}{\partial \theta}+\frac{P}{\rho}\left[\frac{1}{r^2}\frac{\partial}{\partial r}(r^2u)+\frac{1}{r\sin\theta}\frac{\partial}{\partial\theta}(\sin\theta\, v)\right]$$
$$+\frac{1}{\rho}\left[\frac{1}{r^2}\frac{\partial}{\partial r}(r^2F_r)+\frac{1}{r\sin\theta}\frac{\partial}{\partial\theta}(\sin\theta\, F_\theta)\right]=0. \quad (5)$$

The gravitational potential Φ is related to the density ρ through the Poisson equation

$$\nabla^2\Phi=\frac{1}{r^2}\frac{\partial}{\partial r}\left(r^2\frac{\partial\Phi}{\partial r}\right)+\frac{1}{r\sin\theta}\frac{\partial}{\partial\theta}\left(\sin\theta\frac{1}{r}\frac{\partial\Phi}{\partial\theta}\right)=4\pi G\rho. \quad (6)$$

In equation (5), F_r and F_θ are the energy fluxes carried by radiation in the r and θ directions respectively. As in the spherical case, we have considered it an adequate approximation to relate the radiative energy flux to the local temperature gradient by using the radiative diffusion equation; we then have

$$F_r=-\frac{16\pi\sigma T^3}{3\kappa\rho}\frac{\partial T}{\partial r}, \qquad F_\theta=-\frac{16\pi\sigma T^3}{3\kappa\rho}\frac{1}{r}\frac{\partial T}{\partial\theta}. \quad (7)$$

The possible occurrence of shock fronts in the flow has been allowed for by means of the standard artificial viscosity method, generalized to two dimensions as described in the Appendix. Although incipient shock fronts are sometimes encountered in the calculations, they do not appear to play a major role during the relatively early stages of the collapse studied in this investigation. The manner of constructing difference equations and the methods used in solving them are outlined in the Appendix. In the present method, gravitational forces are obtained by solving the Poisson equation (6) simultaneously with the other equations at each time step. The only complication in using the Poisson equation is that boundary values of the potential Φ must be specified at all points on the boundary at each time step. In some of the preliminary calculations, approximate values for Φ at the boundary were computed on the assumption that all of the mass in the cloud is concentrated at the centre; later, accurate boundary values for Φ were computed by integrating over the mass distribution at each time step. This made almost no difference to the results; thus the accurate specification of boundary values for Φ does not appear to be of crucial importance for the results.

Because of the strong demands on computer time and storage made by the two-dimensional calculations, the calculations have so far been made only with very coarse numerical grids. Also, it was thought that it would be more instructive to be able to run many numerical experiments of low or moderate accuracy, rather than only a few of high accuracy; again, a coarse grid is dictated. Most of the calculations have been made with a 12×6 grid, with 12 subdivisions in the radial (r) direction and 6 in the angular (θ) direction. (We assume symmetry with respect to the equatorial plane $\theta=\pi/2$, so that only the interval $0\leqslant\theta\leqslant\pi/2$ is considered.) Needless to say, it is difficult to attain anything approaching quantitative accuracy with such a coarse grid; however, considerable effort has been expended in an attempt to ensure that the results are at least qualitatively reliable, and it is believed that this is the case.

3. THE COLLAPSE OF AN AXISYMMETRIC NON-ROTATING CLOUD

In order to investigate numerically whether deviations from spherical symmetry tend to grow indefinitely during the collapse of an isothermal cloud, a number of

calculations have been made for clouds whose initial density distributions deviate from spherical symmetry and are either elongated (prolate) or flattened (oblate). The calculations have all assumed a cloud mass of one solar mass, a radius of 10^{17} cm, and a temperature of the order of 10°K; the average density of the cloud is then $4{\cdot}8\times10^{-19}$ g cm^{-3}, i.e. approximately five times that required by the Jeans criterion, so that gravity should be safely dominant over pressure forces. In most cases it was possible to continue the calculations until the central density reached a value of the order of 10^{-15} g cm^{-3} or higher.

In the first calculations to be tried, the initial density distribution was approximately uniform but was given a small or moderate deformation from spherical symmetry, either prolate or oblate. The results of these calculations revealed no tendency for the initial deviation from spherical symmetry to be magnified during the collapse; the density distribution always remained approximately spherical, and the results were in all respects quite similar to those obtained previously for the collapse of a spherical cloud. An interesting feature of the results was that the (small) deviations from spherical symmetry tended to oscillate between prolate and oblate forms, although usually only half a cycle of the oscillation could be completed before the cloud became highly centrally condensed. Thus an initially prolate density distribution ' rebounded ' into an oblate shape, whereas an initially oblate form rebounded into a prolate shape before rapid central condensation dominated the motion. These results clearly indicate that pressure forces, while not strong enough to prevent collapse, are nevertheless strong enough to maintain approximate spherical symmetry during the collapse and prevent the indefinite growth of small deviations from spherical symmetry.

In view of the above results, some further experiments were undertaken in which the initial density distribution deviated more drastically from spherical symmetry. Two sets of calculations were made, one with an elongated cylindrical initial density distribution, and a second with a flattened plane-parallel initial configuration. In both cases the calculations were repeated with several different assumed temperatures near 10°K in order to investigate the effect of varying the ratio of pressure to gravitational forces. (Changing the temperature by a certain factor is equivalent to leaving the temperature unchanged but changing all lengths by the same factor.) The results of the two sets of calculations are illustrated in Figs 1 and 2 respectively.

Fig. 1(a) illustrates the initial density distribution assumed in the first set of calculations. The initial density distribution is given by

$$\rho_0(r,\theta) = 7{\cdot}8\times10^{-18}[1+(10r\sin\theta/R)^2]^{-1}\ \text{g cm}^{-3}$$

where $R = 10^{17}$ cm is the radius of the cloud; the isodensity contours for this density distribution are then vertical cylinders, as illustrated in Fig. 1(a) for one quadrant of the (r, θ) plane. (In virtue of the assumed symmetries, only one quadrant of the (r, θ) plane need be illustrated; the others may be obtained by reflection about the axes.)

Fig. 1(b) shows the density distribution resulting at a typical time in the collapse ($t = 3{\cdot}9\times10^{12}$ s) when a temperature of 13°K is assumed. In this case the horizontal pressure gradient is sufficient to cause the cloud to expand horizontally and assume an oblate shape; the density distribution remains oblate as the cloud collapses and becomes more centrally condensed, although the density contours appear to become less oblate with time in the central rapidly collapsing

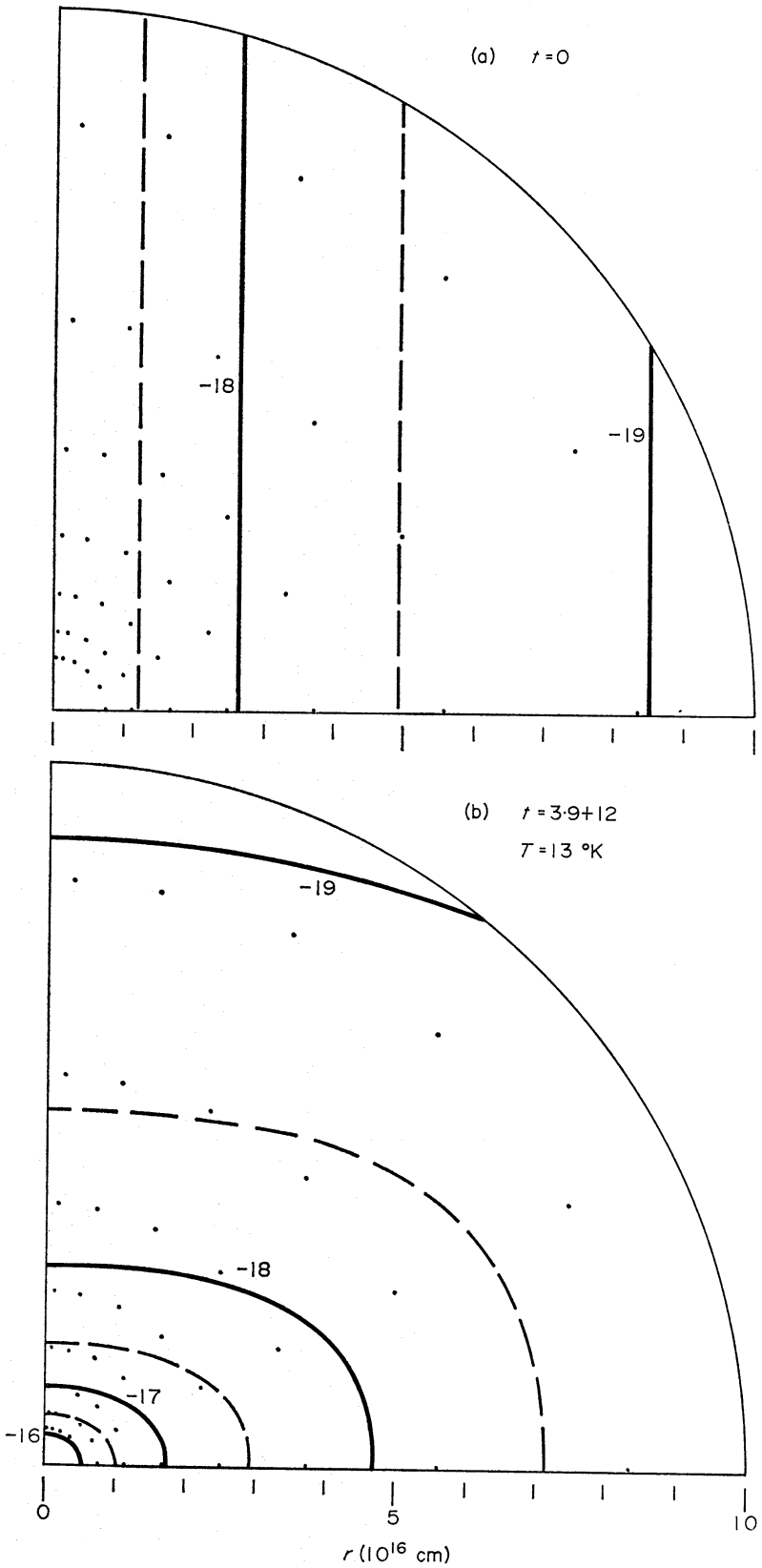

FIG. 1. *Results for the collapse of a cloud with an initially cylindrical density distribution. (a) Density contours for the initial density distribution; (b) density contours after* $3{\cdot}9 \times 10^{12}$ *s for* $T = 13\,°K$*; (c) density contours after* $2{\cdot}6 \times 10^{12}$ *s for* $T = 10\,°K$*; (d) density contours after* $2{\cdot}1 \times 10^{12}$ *s for* $T = 7{\cdot}5\,°K$*. Solid curves refer to integral values of log density, as marked; dashed curves are for half-integral values. Dots indicate the grid points at which densities are calculated.*

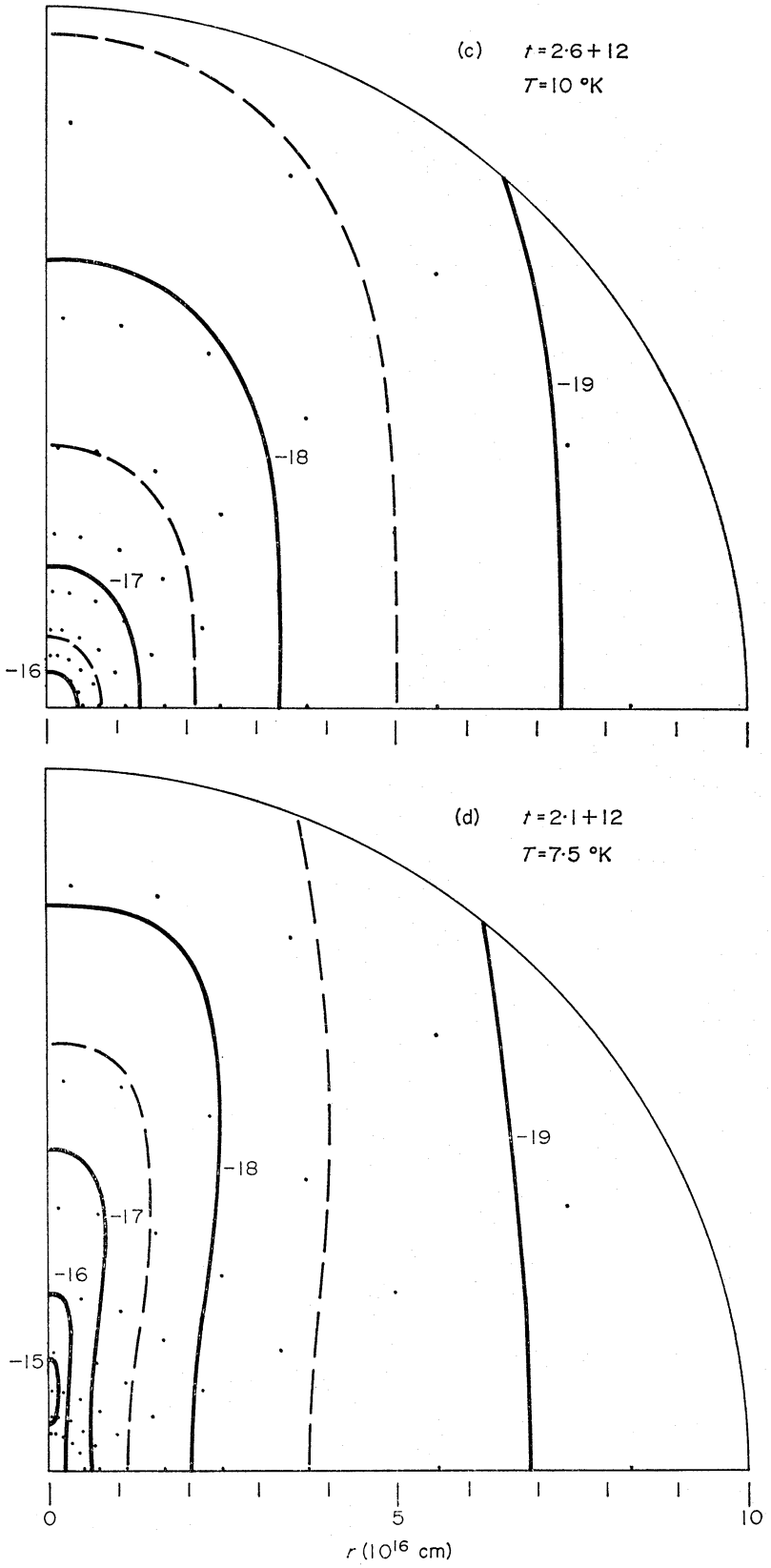

FIG. 1—*continued*

part of the cloud. Fig. 1(c) shows the result obtained when a temperature of 10 °K is assumed; in this case the horizontal pressure gradient is less important and the cloud retains a prolate shape, although the density distribution in the central part of the cloud becomes very nearly spherical as the collapse proceeds. Finally, Fig. 1(d) shows the result obtained when a temperature of 7·5 °K is assumed. In this case the horizontal pressure gradient is insufficient to prevent collapse in the horizontal direction, and the cloud begins to collapse toward a very thin spindle. At the same time, however, the cloud develops two density maxima somewhat removed from the centre along the vertical axis (at $r \sim 10^{16}$ cm); it appears that the cloud has begun to fragment into two subcondensations.

These results can be understood by comparing the assumed initial conditions with those required for the equilibrium of an isothermal cylinder. According to Ostriker (1964a) and Mestel (1965a), a cylindrical equilibrium configuration is possible only if the mass per unit length along the cylinder has the unique value

$$\frac{M}{L} = \frac{2\mathscr{R}T}{G}. \tag{8}$$

It is expected (Mestel 1965a) that if the line density of a cylindrical mass distribution is smaller than this critical value the cylinder will expand indefinitely, whereas if the line density exceeds this value the cylinder will collapse indefinitely toward its axis. For the mass distribution illustrated in Fig. 1(a), the value of M/L is about $1{\cdot}0 \times 10^{16}$ g cm^{-1}, whereas the values of $2\mathscr{R}T/G$ are about $1{\cdot}3 \times 10^{16}$, $1{\cdot}0 \times 10^{16}$, and $7{\cdot}6 \times 10^{15}$ g cm^{-1} for the assumed temperatures of 13, 10, and 7·5 °K. Thus for $T = 13$ °K, the cylindrical mass distribution should begin to expand laterally; for $T = 10$ °K, pressure and gravity should nearly balance, whereas for $T = 7{\cdot}5$ °K the cylinder should begin to collapse indefinitely toward its axis. In all cases there is nothing to prevent collapse in the vertical direction, so that even if the line density is initially below the critical value (8), collapse in the vertical direction eventually brings it above this value, thus ensuring collapse in the horizontal direction as well. Once the cloud has begun to collapse in both coordinates, the form of the density distribution (i.e. its prolateness or oblateness) does not appear to change greatly, except in the case with $T = 7{\cdot}5$ °K, where a tendency toward fragmentation is observed.

The tendency for a thin collapsing cylinder to break into fragments along its length is expected from an elementary application of the Jeans criterion (McCrea 1957). While there appears to be no detailed stability analysis for an isothermal cylinder, the Jeans length for such a cylinder is comparable with its thickness, so that fragmentation would be expected to occur on length scales comparable to or greater than the thickness of the cylinder. On this basis, one would expect the cloud to fragment into at least two subcondensations in the case illustrated in Fig. 1(d).

Fig. 2(a) shows the initial density distribution assumed in the second set of calculations, the results of which are illustrated in Fig 2(b)–(d). The initial density distribution is given by

$$\rho_0(r, \theta) = 2{\cdot}3 \times 10^{-18}[1 + (10r \cos \theta/R)^2]^{-1} \text{ g cm}^{-3},$$

and the initial density contours are horizontal planes, as shown in Fig. 2(a). Fig. 2(b), (c) and (d) illustrate the results obtained when temperatures of 12·5, 10 and 5 °K are assumed. With $T = 12{\cdot}5$ °K, the vertical pressure gradient is

strong enough to make the cloud expand vertically and assume a prolate shape, as seen in Fig. 2(b); in the central part of the cloud, however, the density distribution becomes more nearly spherical as the collapse proceeds. When $T = 10°K$ there is less vertical expansion, and the outer density contours become almost spherical, as seen in Fig. 2(c); in this case, however, the density distribution in the central part of the cloud becomes elongated, and its prolateness increases steadily as the collapse proceeds. When $T = 5°K$, as in Fig. 2(d), pressure gradients are insufficient to halt collapse in the vertical direction (except for a short time at the beginning of the calculations), and the density distribution remains quite oblate during the collapse, although the oblateness appears to decrease gradually in the central part of the cloud as the collapse proceeds.

The fact that the density distribution in the central part of the cloud becomes steadily more elongated in the case with $T = 10°K$ (Fig. 2(c)) may be understood from the fact that in this case the material remains concentrated near the equatorial plane, so that when the cloud collapses horizontally to form a prolate configuration, the line density in the prolate configuration exceeds the critical value (8). The prolate configuration then cannot resist indefinite collapse toward its axis, and the later development of the density distribution in the central region will presumably resemble that seen in Fig. 1(d). In the case of a very flattened density distribution, as in Fig. 2(d), there is no corresponding possibility for rapid collapse to an infinitely thin disc, since there always exists an equilibrium configuration for any value of the surface density (Spitzer 1942; Ledoux 1951). In the case illustrated in Fig. 2(d), collapse in the vertical direction is in fact significantly retarded by pressure gradients, and continuing vertical contraction is made possible mainly by the increasing surface density produced by collapse in the horizontal direction. Since the horizontal collapse is, as always, non-homologous, the horizontal extent of the rapidly collapsing ' core ' of the cloud shrinks just as rapidly as the vertical extent, so that the oblateness of the density distribution remains approximately constant, instead of increasing steadily with time as predicted by Mestel (1965a) on the assumption of homologous collapse in the horizontal direction.

Summarizing the results of this section, we find that even when the assumption of spherical symmetry is relaxed, the behaviour of a collapsing cloud is generally very similar to what was previously found for a spherically symmetric cloud. The collapse is in all cases very non-homologous, and the cloud develops a strong central condensation, just as in the spherical case; also, except for the most extreme deviations from spherical symmetry, as in Fig. 1(d), the radial density variation is roughly of the form $\rho \propto r^{-2}$ in both the horizontal and vertical directions. The numerical results show no tendency for small deviations from spherical symmetry to be magnified during the collapse, provided that the initial conditions are roughly in accordance with the Jeans criterion. Even large deviations from spherical symmetry are usually not amplified during the collapse; this was found to occur only in the case of a prolate mass distribution whose line density exceeds the critical value (8). In this case, however, the elongated cloud becomes unstable to fragmentation into smaller condensations along its length as it collapses.

An important implication of these results is that, contrary to most previous expectations, an isothermal and roughly spherical cloud generally does *not* become unstable to fragmentation as it collapses gravitationally; such a cloud usually collapses into a single central condensation and does not develop more than one density maximum. Fragmentation can occur, but it appears from the present results

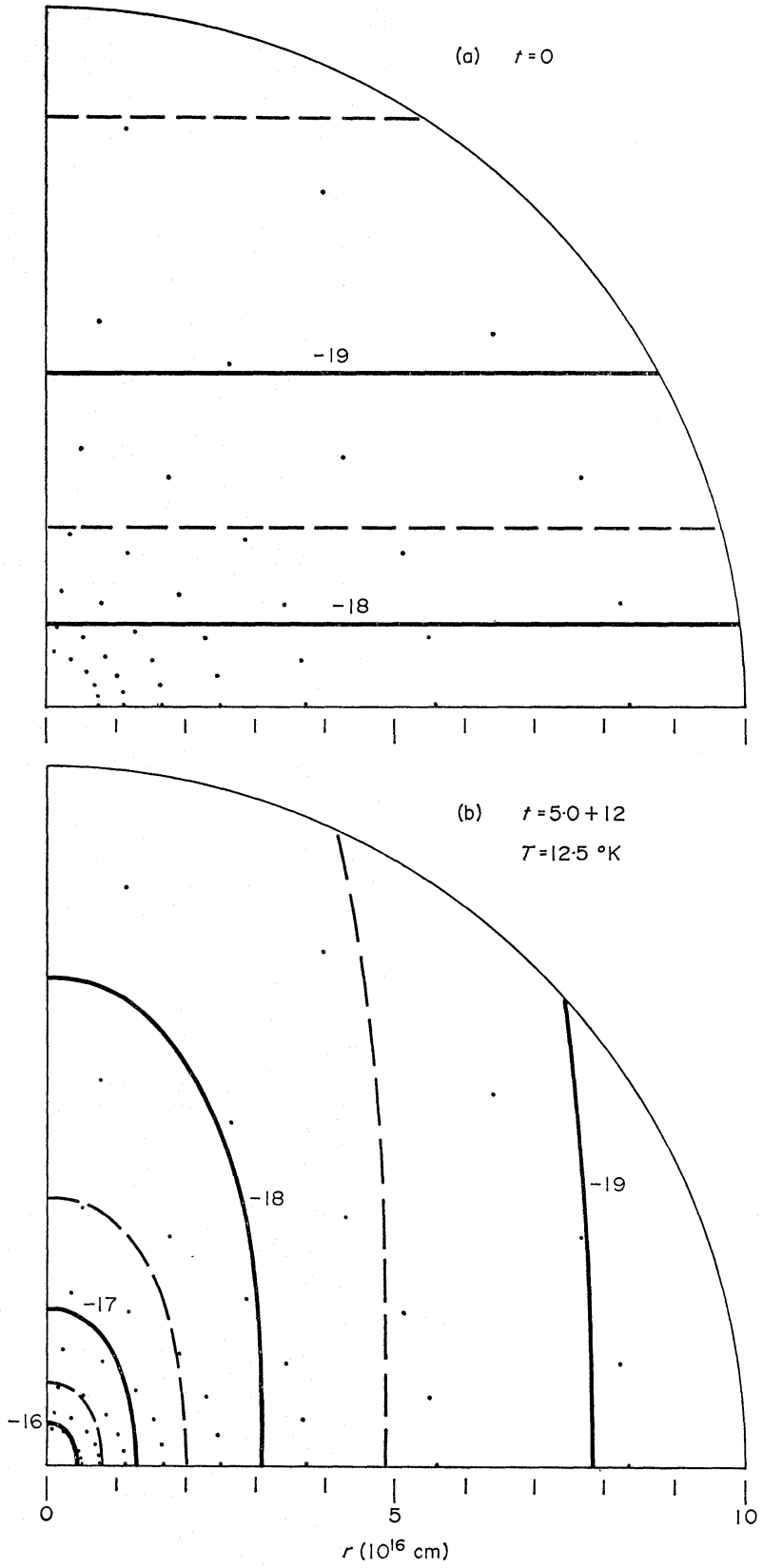

FIG. 2. *Results for the collapse of a cloud with an initially plane-parallel density distribution. (a) Density contours for the initial density distribution; (b) density contours after* $5{\cdot}0 \times 10^{12}$ *s for* $T = 12{\cdot}5\,°K$*; (c) density contours after* $3{\cdot}7 \times 10^{12}$ *s for* $T = 10\,°K$*; (d) density contours after* $2{\cdot}7 \times 10^{12}$ *s for* $T = 5\,°K$.

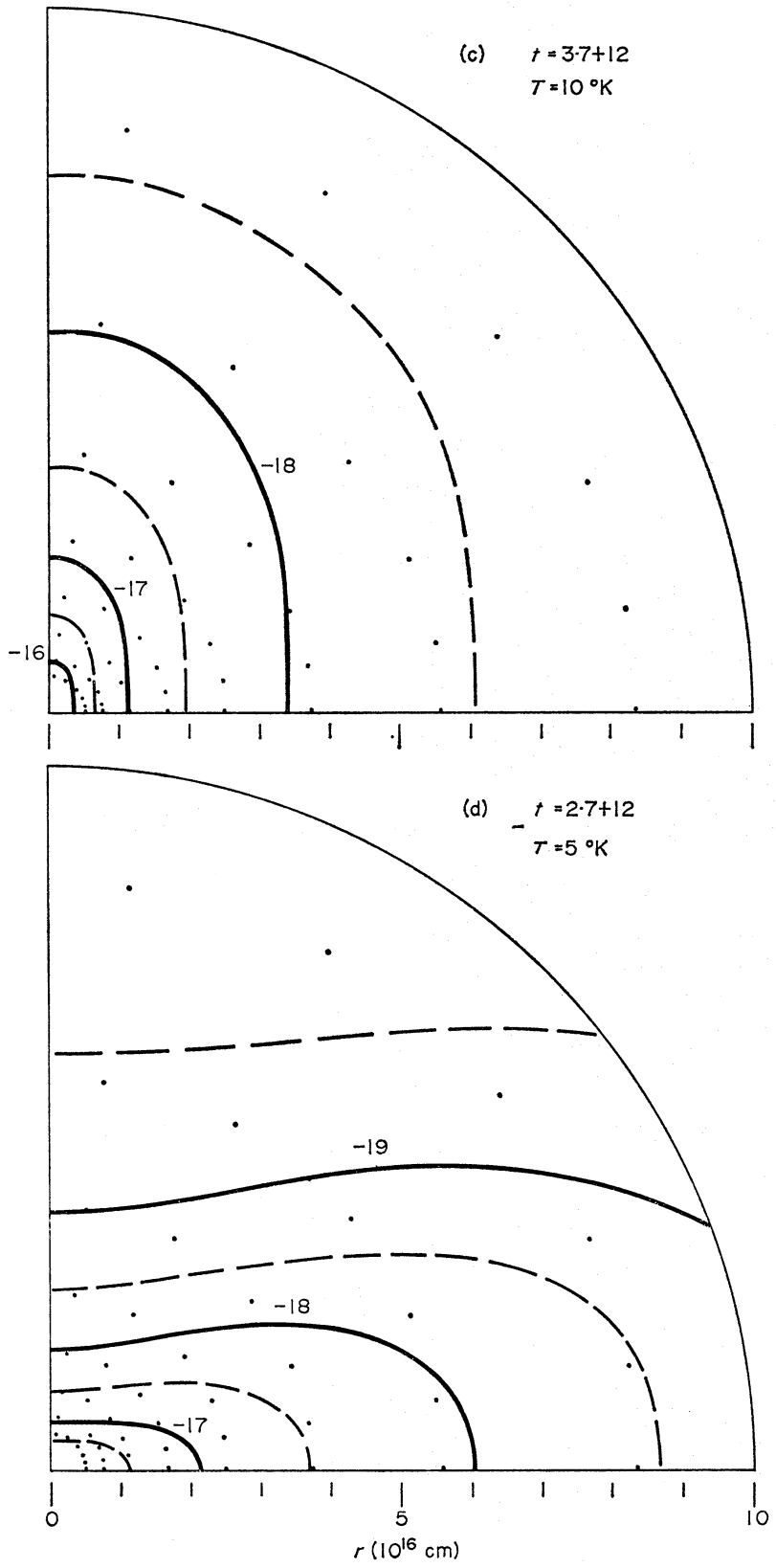

FIG. 2—*continued*

that this will happen only with somewhat special initial conditions such that a tendency toward fragmentation is either present initially or arises at an early stage in the collapse. Classical discussions of the fragmentation problem (e.g. Mestel 1965a) have usually assumed that the overall collapse of the cloud is roughly homologous; in this case, pressure forces become less and less important as the collapse proceeds, allowing fragmentation into smaller and smaller subcondensations to occur. In reality, however, we find from the numerical calculations that the collapse is always quite non-homologous, and that because of this, pressure forces generally remain sufficiently important during the collapse to inhibit fragmentation and prevent the growth of large deviations from spherical symmetry. We shall discuss the implications of this result again in Section 5; meanwhile, we proceed in Section 4 to consider the effect of rotation on the collapse.

4. THE COLLAPSE OF A ROTATING CLOUD

The calculations of the collapse of a rotating cloud have all been made for a mass of one solar mass and a temperature of 10°K. Most of the calculations have been made with a cloud radius of 10^{17} cm, but other values have also been tried. In all cases, the initial density distribution has been assumed to be uniform, and the cloud has been assumed to start with uniform (solid body) rotation. Since the primary purpose of these calculations has been to investigate the effects of rotation on the collapse, the cloud has usually been given an initial angular velocity sufficient to make the effects of rotation become important at a relatively early stage in the collapse. According to the discussion in the Introduction, it is likely that this will commonly be the case.

In carrying out the calculations, it was soon found that the results were quantitatively very sensitive to the conservation or non-conservation of angular momentum during the collapse. Since it is impossible to conserve the angular momentum of each fluid element exactly with an Eulerian method, some numerical inaccuracies are bound to arise, particularly with the present coarse grid. In an effort to ensure that the results are nevertheless qualitatively reliable, considerable experimentation has been done with modifications to both the difference equations and the grid structure. In all cases the results obtained were qualitatively similar, except for a few cases where it was obvious that large errors were present. On the basis of this experience, it is believed that the results are qualitatively correct, and that quantitative errors do not usually exceed a factor of 2.

The first result to be found from the collapse calculations was that the cloud can collapse only if its initial angular velocity ω_0 is smaller than a certain critical value which depends on the cloud radius R; if ω_0 exceeds this value, the cloud does not collapse but settles into a stable equilibrium configuration with only moderate flattening and central concentration. Another way of stating this result is that for any given value of ω_0, there is a critical value of the cloud radius R, such that the cloud will collapse only if its radius is smaller than this critical value. The critical radius depends inversely on ω_0, so that the higher the angular velocity, the more compressed the cloud must be in order for collapse to occur. Thus the presence of rotation modifies the Jeans criterion, and a generalized form of the Jeans criterion must take into account the effects of both pressure and centrifugal forces in inhibiting gravitational collapse.

A number of trial collapse calculations were made in order to determine the

critical angular velocity ω_c for a number of different values of R. The results are shown in Table 1, where R is expressed in terms of $R_m = 1{\cdot}7 \times 10^{17}$ cm, the approximate maximum value of R for which collapse can occur in the absence of rotation (cf. Larson 1969, where a more accurate value of $1{\cdot}83 \times 10^{17}$ cm was determined), and ω_c is expressed in terms of $\omega_m = (4\pi G\rho_0/3)^{1/2}$, the value of ω_0 for which centrifugal force and gravity initially just balance in the equatorial plane.

TABLE I

R (cm)	R/R_m	ω_c (s^{-1})	ω_c/ω_m
1·0 (+17)	0·59	~3·2 (−13)	~0·9
1·4 (+17)	0·82	~1·1 (−13)	~0·5
1·63 (+17)	0·96	~3·3 (−14)	~0·2

It was attempted to find a simple approximate formula which would represent the numerical results in Table I and serve as an approximate generalization of the Jeans criterion for the case of a rotating cloud. Within the (low) accuracy of the results, we find that a rotating cloud with a fixed boundary will collapse if the following condition is satisfied:

$$E_R \lesssim 0{\cdot}42\,\frac{GM}{R} - \mathscr{R}T \quad \text{or} \quad R \lesssim 0{\cdot}42\,\frac{GM}{\mathscr{R}T + E_R}, \tag{9}$$

where

$$E_R = \tfrac{1}{5}\omega^2 R^2$$

is the rotational kinetic energy of the cloud per unit mass. We note that $\mathscr{R}T$ is just two-thirds of the thermal kinetic energy per unit mass, and may be thought of as the kinetic energy of thermal motions parallel to the equatorial plane; thus the rotational and thermal kinetic energies for motions parallel to the equatorial plane are roughly additive in their effects in inhibiting the collapse of the cloud. We note also that a stability criterion similar in form to (9), but with somewhat different numerical coefficients, was derived by Chandrasekhar (1961) for the case of an infinite, uniform, and uniformly rotating medium.

If condition (9) is satisfied and the rotating cloud does collapse, its behaviour is found to be qualitatively much the same in all cases, regardless of the exact choice of R or ω_0 (provided that ω_0 is not too small). At first, gravity dominates and the cloud begins to condense centrally in much the same way as is found for a non-rotating cloud. As the material falls inward the rotational velocity increases, as required by the conservation of angular momentum, and the density distribution becomes flattened toward the equatorial plane, particularly near the centre of the cloud where the density and the rotational velocity increase most rapidly with time. Eventually, after a time depending on the initial angular velocity, centrifugal forces in the central part of the cloud begin to exceed gravity, and collapse perpendicular to the axis of rotation is halted near the centre of the cloud. Meanwhile, collapse along the axis of rotation, which is not inhibited by centrifugal forces, continues unimpeded until nearly all of the material near the axis of rotation has fallen into the central part of the cloud.

After most of the low angular momentum material near the axis of rotation has fallen into the centre of the cloud, the central density stops increasing and even begins to decrease as the material rebounds outward in the equatorial plane. At the same time, material from the outer part of the cloud continues to fall inward and accumulate in a ring-shaped region around the periphery of the central region where the collapse has been halted. The density builds up rapidly in this ring-shaped region, while the central density continues to decrease, so that the density distribution begins to resemble a ' doughnut ' with a density minimum at the centre. Once such a ' doughnut ' or ring has begun to form, the gravitational attraction of the ring draws more and more material into it, and the ring becomes steadily more massive and more condensed.

Fig. 3 illustrates the result of a typical calculation, made assuming a cloud radius of 10^{17} cm and an initial angular velocity of $3{\cdot}0 \times 10^{-13}$ s^{-1}, roughly 10 per cent less than the critical angular velocity $\omega_c \simeq 3{\cdot}2 \times 10^{-13}$ s^{-1}. The results are shown for a time $1{\cdot}2 \times 10^{13}$ s or about four free-fall times after the beginning of the collapse; by this time the ring has become well marked and contains about 15 per cent of the total mass of the cloud. Fig. 3(a) and (b) show the density contours in one quadrant of the (r, θ) plane, where the vertical axis is the axis of rotation; Fig. 3(b) is an enlargement of the central part of Fig. 3(a) to show more clearly the ring, whose radius is only about 5 per cent of the radius of the cloud. Fig. 3(c) and (d) show the velocity vectors at each grid point, projected onto the meridional plane. Fig. 3(c) shows clearly that the cloud collapses much more strongly along the axis of rotation than in the perpendicular direction, and Fig. 3(d) shows that in the central part of the cloud the material is all falling into the ring. In the vicinity of the ring the rotational velocity w, which is not illustrated, increases with increasing distance from the centre, reaching a maximum value of about 0·6 km s^{-1} at a radius $r \simeq 7 \times 10^{15}$ cm, which is approximately at the outer edge of the ring.

The formation of a ring appears to be a very general result of the collapse of a rapidly rotating cloud, since this result was found in nearly all of the calculations tried, and even in a few cases where the effects of rotation did not become important until the central part of the cloud had become opaque; in these cases, the material in the ring attained densities above 10^{-11} g cm^{-3} and temperatures above 100°K. The non-homologous nature of the collapse appears to play an important role in the formation of the ring, since this causes the collapse to be halted and reversed first at the centre of the cloud, while material farther from the centre continues to fall inward and accumulate in a ring-shaped region around the periphery of the expanding central region. However, even apart from the details of the collapse process, it is not surprising that a ring should appear, since it is known that a flattened rotating disc is subject to numerous instabilities, both axisymmetric and non-axisymmetric (Hunter 1963). In the present calculations, where axial symmetry is assumed, only the axisymmetric or ' ring mode ' instabilities can appear. The Maclaurin spheroids are known to become secularly unstable to the formation of a ring when the ratio of thickness to diameter becomes less than about one-sixth (Bardeen 1971); this degree of flattening agrees roughly with that observed in the central part of the cloud when the ring begins to appear. Thus it is probably to be expected that a ring will form just as a result of the ring mode instability of a rotating disc, if for no other reason; it is worth noting, however, that in the present calculations the ring begins to form during the dynamical collapse phase, before any equilibrium disc has been formed.

The radius of the ring is not accurately determined in the present calculations, but the results nevertheless show clearly that the ring radius is very sensitive to the initial angular velocity ω_0, being roughly proportional to ω_0^3. Also, the structure and evolution of the ring are not accurately calculated but it is clear that the ring tends to collect a substantial part of the total mass of the cloud (more than half, in some cases), and to become thinner and more condensed as it grows in mass; the thickness of the ring eventually becomes less than 10 per cent of its radius. In addition, the radius of the ring tends to shrink with time. Within the accuracy of the calculations, the properties of the ring appear to agree approximately with those derived for thin isothermal rings by Ostriker (1964b).

An important property of the isothermal rings studied by Ostriker (1964b) is that for an equilibrium isothermal ring there is a unique value for the mass per unit length which is the same as that for an isothermal cylinder, as given in equation (8). In the present calculations, the line density of the ring happens to be approximately equal to the critical value (8) at the time represented by Fig. 3, but it continues to increase to higher values as the ring accretes more material. When the line density exceeds the critical value, no equilibrium configuration is possible; the ring must collapse to an infinitely thin hoop, and according to the formulas of Ostriker, the radius of the ring must at the same time shrink indefinitely. In reality, this predicted behaviour of the ring will almost certainly not occur, since such a thin collapsing ring would almost certainly be highly unstable to non-axisymmetric perturbations and would break up into fragments, perhaps in much the same way as the thin isothermal cylinder studied earlier. The ultimate outcome of the collapse of a rapidly rotating cloud would then be the formation of a system of two or more condensations orbiting around each other.

It is likely, in fact, that non-axisymmetric instabilities will arise in the collapsing cloud even before a well-defined ring has been formed. This is suggested by the fact that Goldreich & Lynden-Bell (1965b) found that a rotating gaseous configuration can become unstable to the growth of non-axisymmetric perturbations even before the axisymmetric ring mode instabilities appear. Also, it is known that the Maclaurin spheroids become unstable to non-axisymmetric deformations before becoming unstable to the axisymmetric modes (Lyttleton 1953). Thus it may well be that in reality a ring never forms at all, and the cloud condenses directly into a system of two or more condensations orbiting around each other. This type of result is also suggested by the work of Arny (1967). The ring found in the present calculations would then be just an artifact of the assumption of axial symmetry, i.e. an artificially axisymmetrized form of a more realistic non-axisymmetric configuration consisting, for example, of two condensations orbiting around each other.

In any case, whether or not a ring ever forms, it appears inescapable that the ultimate outcome of the collapse of a rapidly rotating cloud will be the formation of a binary or multiple system of condensations orbiting around each other. Since fragmentation into a binary system is the simplest possibility and represents the lowest order deviation from axial symmetry, one might expect that this would be the most frequent outcome of the collapse. This possibility is reminiscent of classical results in the theory of equilibrium configurations for rotating incompressible fluids (Lyttleton 1953) which suggest that fission into a binary system may eventually occur as the density of such a rotating equilibrium configuration is gradually increased. In the present situation, however, we are envisioning not a

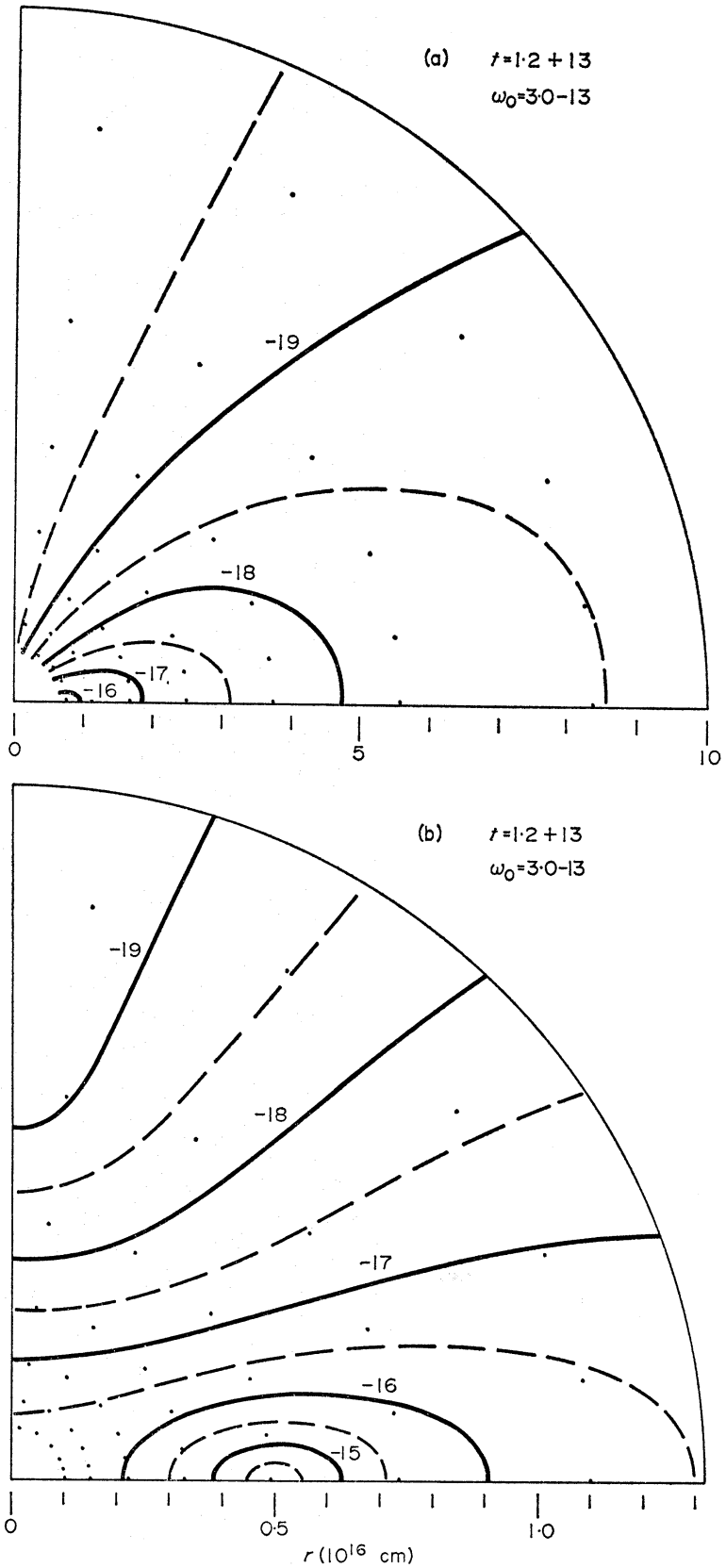

FIG. 3. *Results for the collapse of an initially uniform and uniformly rotating cloud with initial angular velocity* $\omega_0 = 3{\cdot}0 \times 10^{-13}\ s^{-1}$. (*a*) *Density contours for the outer part of the cloud after* $1{\cdot}2 \times 10^{13}\ s$; (*b*) *an enlargement* (7·6×) *of the central part of Fig.* 3(*a*) *showing*

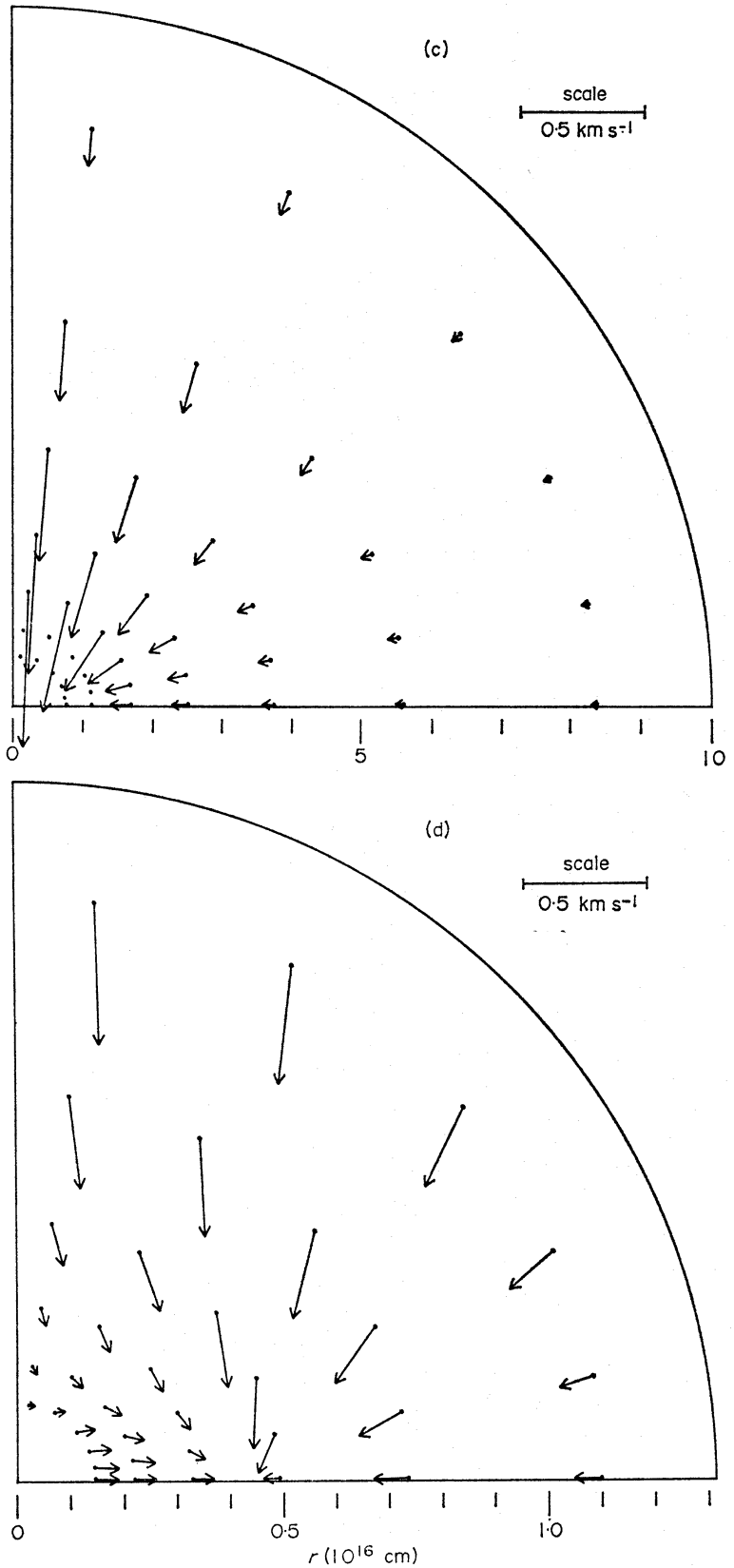

the density contours in the inner part of the cloud; (c) the velocity vectors corresponding to Fig. 3(a), projected into the meridional plane; (d) the velocity vectors corresponding to Fig. 3(b). Solid curves refer to integral values of log density, as marked; dashed curves are for half-integral values. Dots indicate the grid points at which densities are calculated.

fission process but a condensation process in which two or more centres of condensation are formed orbiting around the centre of the cloud.

It is clear that once a rotating collapsing cloud becomes unstable to non-axisymmetric deformations, the two-dimensional (axisymmetric) computing method used in the present calculations is no longer adequate to follow the further development of the cloud, and a full three-dimensional treatment becomes necessary. This is the primary reason why it has not been attempted in the present calculations to follow the collapse of a rotating cloud much beyond the point where a well-defined ring is formed and non-axisymmetric instabilities seem likely to arise (if they have not already appeared).

5. DISCUSSION

The results described in the previous sections have important implications for our understanding of fragmentation and star formation. First, it appears from the results of Section 3 that in the absence of rotation an isothermal cloud does not in general become unstable to fragmentation as it collapses gravitationally; if the initial conditions approximately satisfy the Jeans criterion, and if the cloud is initially roughly spherical, then pressure forces remain sufficiently important during the collapse to maintain approximate spherical symmetry and prevent fragmentation. Fragmentation can occur, but usually only in circumstances where the initial configuration is already unstable toward fragmentation, as was the case for the calculation illustrated in Fig. 1(d). As we have seen in Section 3, this somewhat unexpected result arises because of the unavoidable non-homologous nature of the collapse.

It is still possible, of course, that fragmentation may occur in circumstances where the temperature of the material decreases rapidly as the density rises; such a situation was found by Hunter (1969) and by Disney *et al.* (1969) for the early stages of collapse of a very massive, tenuous interstellar cloud. However, near isothermality is expected to prevail at densities greater than about 10^{-21} g cm^{-3}; this is still too low a density to allow fragmentation into condensations with masses in the normal stellar mass range.

A further difficulty for fragmentation in a non-rotating cloud arises from the fact that even if separate subcondensations do begin to form, as in Fig. 1(d), there is nothing to prevent them from falling together and merging into a single condensation; thus it is not clear that permanent fragmentation can occur at all. In any case, it would seem that fragmentation will at least be inhibited in the absence of any rotational or turbulent motions to prevent the fragments from falling together and merging.

From the results of Section 4, we see that the situation is quite different if the cloud is rotating rapidly. In this case, unless magnetic torques are strong enough to damp out rotational motions on a time scale less than the free-fall time, deviations from spherical symmetry are steadily magnified during the collapse, and it appears very likely that the central part of the cloud will eventually fragment into a system of two or more condensations orbiting around each other. If so, we see that, instead of inhibiting the fragmentation of a collapsing cloud, rotation will in fact have the opposite effect of promoting fragmentation (provided, of course, that the amount of rotation is not large enough to prevent collapse altogether). In view of the conclusion reached above that fragmentation will usually not occur in an

initially quiescent, non-rotating cloud, it thus appears that rotation plays an important role in enabling fragmentation to occur, and may in fact be the primary cause of fragmentation.

Layzer (1963) has argued that permanent fragmentation cannot occur since, according to Layzer, the further contraction of any fragments that form will be prevented by their intrinsic rotational motions, and they will therefore merge and be obliterated during the continuing overall collapse or flattening of the cloud. The present results for the collapse of a rotating cloud show, however, that the presence of rotation can halt collapse perpendicular to the axis of rotation, but cannot prevent some parts of the cloud (i.e. the material in the ring) from permanently attaining densities much higher than the average density of the cloud. If the ring breaks into fragments, as seems likely, the fragments will be prevented by their orbital motions from falling together and merging, so that permanent fragmentation is indeed possible. The prospects for fragmentation should, if anything, be even better if the cloud is not constrained to remain axially symmetric, as in the present calculations, since this constraint prevents the material from becoming as condensed as it might otherwise become, should it prefer to condense directly into two or more orbiting centres of condensation without first forming a ring.

If the final outcome of the collapse of a rapidly rotating cloud is the formation of a binary or multiple system of stars, this would largely dispose of the classical ' angular momentum problem ', since much of the initial angular momentum of the cloud can go into the orbital angular momentum of the stars. It would then seem less necessary to invoke magnetic forces to remove angular momentum from the cloud, as has often been done. In addition, we would obtain an attractive explanation of the fact that most of the stars in the sky are in fact found in binary or multiple systems (Heintz 1969). We note that if the ring illustrated in Fig. 3(b) were to fragment into a binary system with the same angular momentum, the separation of the resulting binary would be about 10^3 A.U., comparable with that of a wide visual binary. Since the radius of the ring is very sensitive to the initial angular velocity of the cloud (approximately proportional to ω_0^3), a binary with a much smaller separation can be formed if the cloud starts out with a smaller angular velocity. Also, a close binary can result from a later stage in the fragmentation of a rapidly rotating cloud (see below).

While it thus appears that the formation of binary and multiple systems can be accounted for as a result of the collapse of rotating clouds, we have yet to account for the many single stars in the sky. A simple and attractive possibility for explaining the single stars as well as the binary and multiple systems within a common framework arises if a rotating cloud often condenses into a small multiple system containing say, 3 or 4 stars. Numerical n-body calculations such as those of Agekyan & Anosova (1968) and Standish (unpublished) show that such systems are nearly always unstable and rapidly disintegrate, ejecting (single) stars until only a stable binary is left. In this way most of the single stars in the sky might be accounted for. Such a mechanism might also account for the more eccentric binary systems, since the binaries resulting from the disintegration of small multiple systems tend to have large eccentricities (Standish, unpublished). The fact that the frequency of binaries appears to be lower than average among the least massive (red dwarf) stars (Heintz 1969) is consistent with this picture, since the least massive stars in a multiple system are the ones most likely to be ejected and least likely to remain in a stable binary system.

Observational evidence that at least the more massive stars are commonly formed in binary or multiple systems comes from the fact that the O stars, which are very young and recently formed objects, nearly always occur in binary or multiple systems (Blaauw 1961). Single O stars are very rare, except for the ' runaway ' stars, which are nevertheless thought to originate in binary systems which have been disrupted as a result of explosive mass loss from one of the stars (Blaauw 1961). A possible alternative explanation for some of the ' runaway ' stars is that they may have resulted from the dynamical disintegration of close multiple systems of massive stars, in much the same way as we have suggested for the origin of the ' normal ' single stars.

A possibility which we have so far not considered is that the fragments which form during the collapse of a rotating cloud may themselves have substantial rotational motions. The likely angular velocities of the fragments cannot be reliably estimated from the present results; however, in the absence of magnetic or viscous forces, Kelvin's circulation theorem applies (Hunter 1964) and shows that the vorticity of any fluid element must increase as it is compressed. If so, simple arguments suggest that centrifugal forces will be approximately as important for the fragments as they were for the original cloud. The fragments may then subdivide into even smaller condensations, and the fragmentation process may continue in this way through several stages until large optical depths are reached and rising temperatures and pressures inhibit further fragmentation. A final stage of fragmentation can occur after the temperature has become high enough to dissociate H_2 molecules, thus triggering a second phase of dynamical collapse (Larson 1969); fragmentation during this phase would in fact be required to account for the close spectroscopic binaries.

Without undertaking full three-dimensional collapse calculations, it is difficult to make any quantitative predictions about the final outcome of the fragmentation process sketched above. It seems likely, however, that it would eventually lead to the formation of a number of accreting cores or ' embryo stars ' moving around in an extended envelope of uncondensed material which still contains most of the original mass of the cloud (cf. Larson 1969). The embryo stars would continue to accrete material from the surrounding envelope until all of the remaining uncondensed material has either been accreted or blown away by a newly formed O star. This picture might account, at least qualitatively, for the observed mass distribution of the stars; one would expect massive stars to be relatively scarce, for example, since only a few favoured objects will be able to build up very large masses before the accretion process is cut off by exhaustion of the uncondensed material, or, more likely, by the formation of an O star.

Yale University Observatory, New Haven, Connecticut 06520

REFERENCES

Agekyan, T. A. & Anosova, Zh. P., 1968. *Astrofizika*, **4**, 31; English translation in *Astrophysics*, **4**, 11.
Arny, T. T., 1967. *Ann. Astrophys.*, **30**, 1.
Bardeen, J. M., 1971. *Astrophys. J.*, **167**, 425.
Blaauw, A., 1961. *Bull. astr. Inst. Netherl.*, **15**, 265.
Bodenheimer, P. & Sweigart, A., 1968. *Astrophys. J.*, **152**, 515.
Chandrasekhar, S., 1961. *Hydrodynamic and Hydromagnetic Stability*, Clarendon Press, Oxford.

Disney, M. J., McNally, D. & Wright, A. E., 1969. *Mon. Not. R. astr. Soc.*, **146**, 123.
Goldreich, P. & Lynden-Bell, D., 1965a. *Mon. Not. R. astr. Soc.*, **130**, 97.
Goldreich, P. & Lynden-Bell, D., 1965b. *Mon. Not. R. astr. Soc.*, **130**, 125.
Heintz, W. D., 1969. *J. R. astr. Soc. Canada*, **63**, 275.
Hunter, C., 1963. *Mon. Not. R. astr. Soc.*, **126**, 299.
Hunter, C., 1964. *Astrophys. J.*, **139**, 570.
Hunter, C., 1967. *Relativity Theory and Astrophysics, Vol.* 2: *Galactic Structure*, Ed. J. Ehlers, p. 169. American Mathematical Society, Providence, R. I.
Hunter, J. H., 1969. *Mon. Not. R. astr. Soc.*, **142**, 473.
Larson, R. B., 1968. Ph.D. thesis, California Institute of Technology. University Microfilms, Ann Arbor, Mich.
Larson, R. B., 1969. *Mon. Not. R. astr. Soc.*, **145**, 271.
Larson, R. B. & Starrfield, S., 1971. *Astr. Astrophys.*, **13**, 190.
Layzer, D., 1963. *Astrophys. J.*, **137**, 351.
Ledoux, P., 1951. *Ann. Astrophys.*, **14**, 438.
Lin, C. C., Mestel, L. & Shu, F. H., 1965. *Astrophys. J.*, **142**, 1431.
Lynden-Bell, D., 1964. *Astrophys. J.*, **139**, 1195.
Lyttleton, R. A., 1953. *The Stability of Rotating Liquid Masses*. Cambridge University Press.
McCrea, W. H., 1957. *Mon. Not. R. astr. Soc.*, **117**, 562.
Mestel, L., 1965a. *Q. Jl R. astr. Soc.*, **6**, 161.
Mestel, L., 1965b. *Q. Jl R. astr. Soc.*, **6**, 265.
Ostriker, J., 1964a. *Astrophys. J.*, **140**, 1056.
Ostriker, J., 1964b. *Astrophys. J.*, **140**, 1067.
Penston, M. V., 1969. *Mon. Not. R. astr. Soc.*, **145**, 457.
Penston, M. V., 1971. *Contemp. Phys.*, **12**, 379.
Spitzer, L., 1942. *Astrophys. J.*, **95**, 329.
Varga, R. S., 1962. *Matrix Iterative Analysis*. Prentice-Hall, Englewood Cliffs, N.J.

APPENDIX

THE NUMERICAL METHOD

The numerical method used in this project has been designed to represent, as nearly as possible, a generalization to two dimensions of the method previously used for computing the collapse of a spherical protostar (Larson 1968, 1969). In particular, it was desired that in the special case of spherical symmetry the present calculations should reduce identically to the previous ones. Consequently, an implicit Eulerian computational scheme has been adopted, and spherical polar coordinates (r and θ) have been used to define the numerical grid. In the spherical case, Eulerian methods have the advantage over Lagrangian ones that a suitable grid structure can be set up at the beginning and used throughout the calculations without the need for extensive re-zoning. In the two-dimensional case this advantage becomes even more important, since the cells in a Lagrangian grid tend to become highly distorted and stretched out.

As before, the cloud has been divided into a set of concentric shells whose boundaries are arranged such that the ratio of radii of neighbouring shell boundaries is a constant; usually a ratio of about 1·5 has been used (cf. the value of $\sqrt{2}$ used previously). These spherical shells are divided into annular zones by a set of conical surfaces of constant θ; usually the θ values are not equally spaced, but are spaced more closely near the equatorial plane in the case of a flattened density distribution, or near the axis of symmetry in the case of a prolate distribution. The variables of state ρ, T, P, and E, the gravitational potential Φ, and the rotational velocity w are assigned values at the central point of each cell in the (r, θ) plane:

the locations of these central points are indicated by the dots in Figs 1–3. The velocity components u and v are assigned values on the cell boundaries perpendicular to the corresponding directions of motion. The potential gradients and radiative fluxes are also evaluated at the cell boundaries.

The partial differential equations (1)–(6) have been represented by difference equations constructed as far as possible in a manner similar to that used in the spherical case; for example, pressure gradients are replaced by logarithmic pressure differences, and where average values of quantities are required, geometric means are used for the variables of state and arithmetic means are used for the velocities (which can change sign). Artificial viscosity terms are evaluated separately for motions in the u and v directions and are inserted separately in the difference expressions referring to motions in the u and v directions.

Since backward time differences are used to ensure stability, the difference equations are implicit and must be solved by an iterative method. We have used the standard Newton–Raphson technique, which involves linearization of the difference equations and the solution of a large set of linear equations. In the case of two or more space dimensions, the matrix of coefficients no longer has all of its non-zero elements near the diagonal; some non-zero elements occur far from the diagonal. This makes a direct method of solution impractical, and one must resort to iterative methods for solving the linear equations. We have used an alternating direction method (Varga 1962), adapted for the case of six simultaneous differential equations instead of only one. Although some difficulties were encountered in obtaining good convergence with the alternating direction method, in the calculations reported here it was found possible to obtain adequate convergence with 4–6 iterations of the alternating direction method for each of 3–4 Newton–Raphson iterations required in each time step. With a 12×6 grid, it then requires roughly 30 s to compute each time step on an IBM 7094 computer, and a typical collapse calculation requires about 20–30 min.